Exp. Anim. 63(1), 11–19, 2014

—Original—

Characterization of the Skeletal Fusion with Sterility (*sks*) Mouse Showing Axial Skeleton Abnormalities Caused by Defects of Embryonic Skeletal Development

Kouyou AKIYAMA, Kentaro KATAYAMA*, Takehito TSUJI, and Tetsuo KUNIEDA

Graduate School of Environmental and Life Science, Okayama University, 1–1–1 Tsushima-naka, Okayama 700-8530, Japan

Abstract: The development of the axial skeleton is a complex process, consisting of segmentation and differentiation of somites and ossification of the vertebrae. The autosomal recessive skeletal fusion with sterility (*sks*) mutation of the mouse causes skeletal malformations due to fusion of the vertebrae and ribs, but the underlying defects of vertebral formation during embryonic development have not yet been elucidated. For the present study, we examined the skeletal phenotypes of *sks*/*sks* mice during embryonic development and the chromosomal localization of the *sks* locus. Multiple defects of the axial skeleton, including fusion of vertebrae and fusion and bifurcation of ribs, were observed in adult and neonatal *sks*/*sks* mice. In addition, we also found polydactyly and delayed skull ossification in the *sks*/*sks* mice. Morphological defects, including disorganized vertebral arches and fusions and bifurcations of the axial skeletal elements, were observed during embryonic development at embryonic day 12.5 (E12.5) and E14.5. However, no morphological abnormality was observed at E11.5, indicating that defects of the axial skeleton are caused by malformation of the cartilaginous vertebra and ribs at an early developmental stage after formation and segmentation of the somites. By linkage analysis, the *sks* locus was mapped to an 8-Mb region of chromosome 4 between *D4Mit331* and *D4Mit199*. Since no gene has already been identified as a cause of malformation of the vertebra and ribs in this region, the gene responsible for *sks* is suggested to be a novel gene essential for the cartilaginous vertebra and ribs.

Key words: mapping, mutant mouse, skeletal defect

Introduction

Axial skeleton development is a complex process, involving segmentation and differentiation of somites and ossification of vertebrae [21]. Many genes controlling axial skeleton formation of mammals have been identified by investigations using a number of mutant mouse strains showing vertebral abnormalities. These mutant strains include the Brachyury [4], tail-short [19], undulated [27], curly-tail [10], crinkly-tail [15], and pudgy strains [11]. In addition, various mice with targeted disruptions of particular genes have also been reported to exhibit skeletal abnormalities [7, 16, 17, 28, 30]. These mutant mice can serve as useful animal models for investigating the developmental mechanisms of axial skeleton formation. For example, the Brachyury (*T*) strain is one of the most classic mutant mouse strains associated with chromosomal inversion and has a tailless

(Received 17 April 2013 / Accepted 12 June 2013)

Address corresponding: T. Kunieda, Graduate School of Environmental and Life Science, Okayama University, 1–1–1 Tsushima-naka, Okayama 700-8530, Japan

**Present address: Nippon Veterinary and Life Science University*

phenotype in heterozygotes (*T*/+) [4, 24]. The causative gene for Brachyury has been identified as an essential gene in mesoderm formation[14], and this mutant mouse has proven to be an excellent tool for studying the processes underlying mesoderm formation in mammals.

Skeletal fusion with sterility (*sks*), an autosomal recessive mutation in the mouse, arose spontaneously in the A/J strain at Jackson Laboratory. *Sks*/*sks* mice show skeletal fusions of the vertebrae and bilateral or unilateral fusions of the ribs, although the severity of these morphological abnormalities varies depending on genetic background. Both male and female *sks*/*sks* mice are sterile due to defects of gametogenesis [13]. The underlying defects of skeletal formation in the *sks*/*sks* mouse, including defective processes of vertebral formation during embryonic development, have not been fully investigated. In addition, while the *sks* locus has been roughly mapped to a region of mouse chromosome 4 distal to the brown mutation on the tyrosinase-related protein 1 (*Tyrp1*^{b}) gene [13], the exact chromosomal location of the *sks* locus remains to be identified. Therefore, we examined the skeletal abnormality of *sks*/*sks* mice at various developmental stages in order to reveal the precise skeletal defects during development. We also performed linkage analysis using F_2 progeny obtained from a cross between the *sks* and JF1 strains in order to map the location of the *sks* locus on mouse chromosome 4.

Materials and Methods

Mice

The mice used in this study were obtained from the mouse mutant resource colony of the Jackson Laboratory (Bar Harbor, ME, USA), and the strain has been maintained by intercrossing heterozygous mice. The JF1/Ms strain was obtained from the National Institute of Genetics (Mishima, Japan). These animals were given food and water *ad libitum* and maintained under conditions of a 12-h light/12-h dark cycle at a room temperature of 24–26°C. Protocols for the use of animals in the present study were approved by the Animal Care and Use Committee of Okayama University.

Skeletal preparation of adult, newborn, and embryonic mice

Skeletal preparations of adult and newborn mice were made as follows. Mice were euthanized by asphyxiation with CO_2, eviscerated, fixed in 95% ethanol, and stained for cartilage in ethanol/acetic acid (4:1) with 0.025% alcian blue. After clearing of the soft tissues with 1% KOH for 1 h, the mice were stained for bone in 1% KOH and 0.025% alizarin red, destained in 20–70% glycerol containing 1% KOH, and stored in 70% glycerol.

Adult *sks* heterozygous female mice were mated with *sks* heterozygous male mice, and vaginal plugs were checked every morning. When a vaginal plug was observed, the embryonic day (E) was determined as E0.5. To collect embryos, the *sks* heterozygous mice were mated, and the pregnant females were euthanized by asphyxiation with CO_2. Next, the embryos were removed from the uteri. E14.5 embryos were fixed with 95% ethanol and stained for cartilage in ethanol/acetic acid (4:1) with 0.025% alcian blue. After clearing the soft tissues with 1% KOH for 30 min, embryos were stored in 30% glycerol. To prepare the histological sections, E12.5 embryos were fixed by Bouin's solution (picric acid:formaldehyde:acetic acid=15:5:1) for 24 h at room temperature. After dehydration in ethanol, clearing in xylene, and infiltration with paraffin wax, tissues were embedded in paraffin wax and sectioned at 7 μm. Sections were stained with hematoxylin and eosin (H&E).

Linkage mapping

To determine the chromosomal localization of the *sks* locus, we performed linkage analysis using F_2 mice obtained from a cross between *sks* and JF1/Ms mice. Heterozygous (*sks*/+) and JF1/Ms (+/+) mice were mated, and F_1 hybrids carrying the *sks* allele (*sks*/+) were then intercrossed. The genotypes of the *sks*/+ F_1 mice were determined by genotyping of two closely linked microsatellite markers, *D4Mit31* and *D4Mit146*. All F_2 mice were euthanized by CO_2 at eight weeks after birth. F_2 mice showing the tail and rib abnormality were judged as *sks*/*sks*. Testis weights of all F_2 male mice were also measured to confirm the phenotype. Finally, 532 F_2 progeny (*sks*/*sks*:*sks*/+ or +/+=63:469) were obtained. Genomic DNA was prepared from the livers of F_2 mice by phenol/chloroform extraction. To map the *sks* locus, microsatellite maker genotypes were obtained for the 63 affected F_2 mice as follows. PCR was carried out in a 10 μl reaction mixture containing 20 ng genomic DNA, 1.5 mM Mg^{2+}, 100 nM of each primer, 100 μM of each dNTP, and 0.25 Units of *Taq* DNA polymerase (Amersham Bioscience, Piscataway, NJ, USA). The amplification protocol consisted of denaturation at 94°C for 5 min followed by 35 cycles consisting of denaturation at 94°C

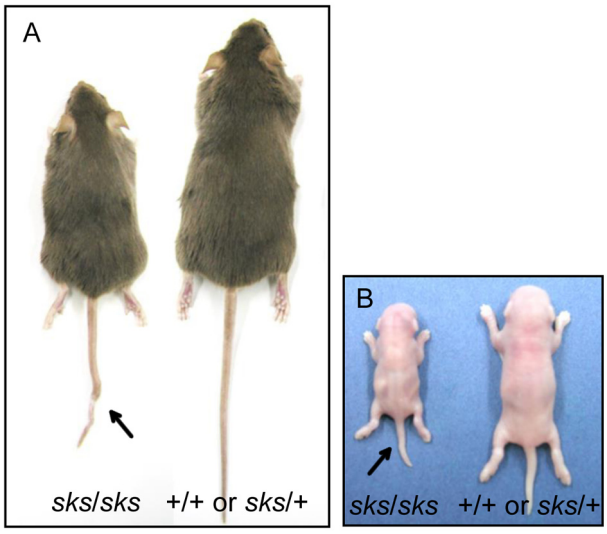

Fig. 1. Gross appearance of the *sks* mutant mice. The gross appearances of *sks*/*sks*(left) and normal (right) mice at 8 weeks of age (A) and postnatal day 1 (B). Tail kinks are indicated by arrows.

for 30 s, annealing at 53–60°C for 30 s, and extension at 72°C for 30 s. Information for the microsatellite markers used in this study is available from UniSTS database under following accession numbers. *D4Mit141* (129917), *D4Mit187* (129968), *D4Mit331* (116523), *D4Mit31* (116521), *D4Mit146* (129922), *D4Mit199* (116299), and *D4Mit332* (116520). The PCR products were electrophoresed on 3% or 4% agarose gels or 6% polyacrylamide gels in 0.5× TAE and stained with ethidium bromide.

To determine the genotype and sex of embryos, genomic DNA was prepared from yolk sacs by phenol/chloroform extraction. The *sks* locus genotype was determined using 2 microsatellite markers, *D4Mit31* and *D4Mit146*, which are closely linked to the *sks* locus. The sex of the embryos was determined as described by Chuma and Nakatsuji [3].

Results

Skeletal abnormalities of adult and neonatal sks/sks mice

The gross appearance of the *sks*/*sks* adult mouse is characterized by a kinky tail and small body size (Fig. 1A). The average body weight of *sks*/*sks* male mice (21.08 ± 0.70 g, n=12) is less than 70% of that of *sks*/+ and +/+ male littermates (31.98 ± 1.03 g, n=13) at 8 weeks of age. The small body size and kinky tail were apparent in neonatal mice shortly after birth (Fig. 1B).

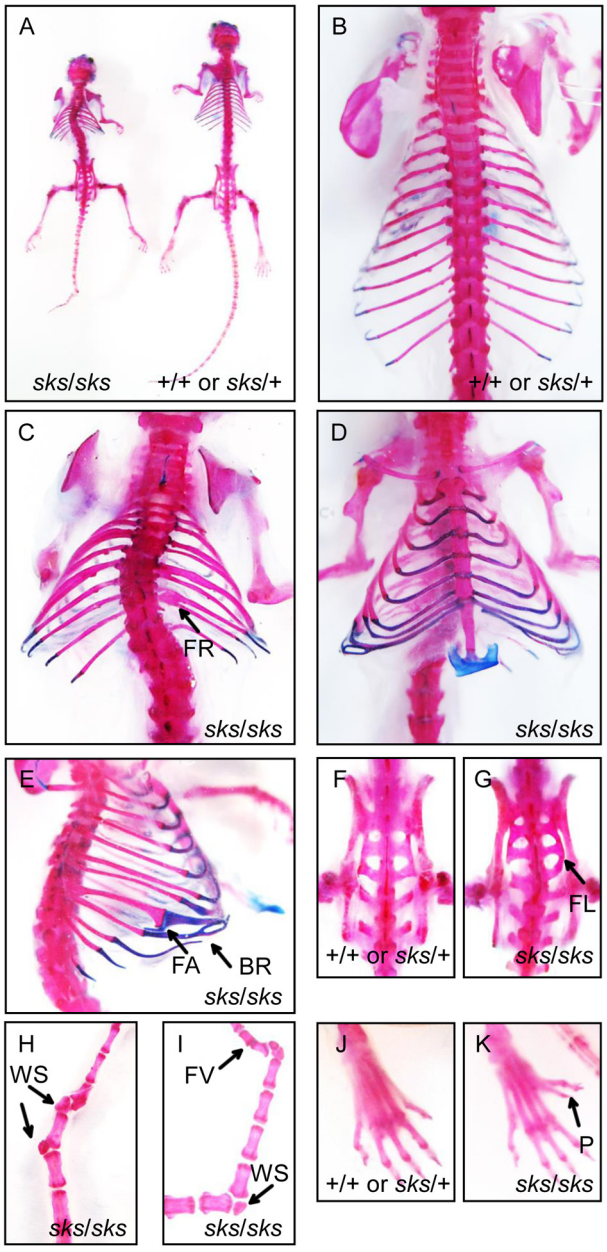

Fig. 2. Skeletal defects of adult *sks* mutant mice. (A) Whole skeleton, (B, C, D, E) thoracic region, (F, G) lumbar region, (H, I) caudal region, and (J, K) hind foot of alizarin red–and alcian blue–stained skeletal preparations of 8-week-old mutant (*sks*/*sks*) and normal (*sks*/+ or +/+) mice. Skeletal malformations are indicated as FR, fused rib; FA, fused arch; BR, branched rib; WS, wedge-shaped bone; FL, fused lumbar; and P, polydactyly.

The axial skeleton of *sks*/*sks* mice showed apparent morphological abnormalities. As shown in Fig. 2, the axial skeleton of *sks*/*sks* mice was bent and severely

disorganized, with multiple skeletal defects in the vertebral column and ribs, including fusion of cervical, thoracic (Fig. 2C and D), lumbar (Fig. 2F and G), and caudal vertebrae (Fig. 2H and I), as well as the fusion and bifurcation of the ribs (Fig. 2E). It was noted that the tail kinks appeared to be caused by wedge-shaped pieces of bone between caudal vertebrae (Fig. 2H and I). In addition, *sks*/*sks* mice often exhibited polydactyly of the hind limb. Four out of seven *sks*/*sks* skeletal preparations showed polydactyly, while none of the eight *sks*/+ or +/+ skeletal preparations showed this abnormality (Fig. 2J and K). As shown in Fig. 3, morphological abnormalities similar to those of the adult mice were apparent in the vertebral column and ribs of neonatal mice at postnatal day 1 (P1). They showed a bent axial skeleton (Fig. 3A), disorganized thoracic vertebrae (Fig. 3C–E), fusion and bifurcation of ribs (Fig. 3C), and a reduced number of ribs (Fig. 3D). Insufficient and disorganized ossification patterns of the vertebrae were observed. Disorganized cartilaginous caudal vertebrae causing the tail kinks were the most apparent abnormality observed in the axial skeleton of the *sks*/*sks* neonatal mice (Fig. 3F). In the *sks*/*sks* neonatal mice, the frontal and parietal bones of the skull exhibited the calvarial ossification defect (Fig. 3G and H), while the skull bone of *sks*/*sks* adult mice exhibited no abnormality (data not shown), indicating delayed ossification of the skull in *sks*/*sks* mice. All four *sks*/*sks* skeletal preparations showed delayed ossification, while none of seven *sks*/+ or +/+ skeletal preparations showed this abnormality (Fig. 3G and H).

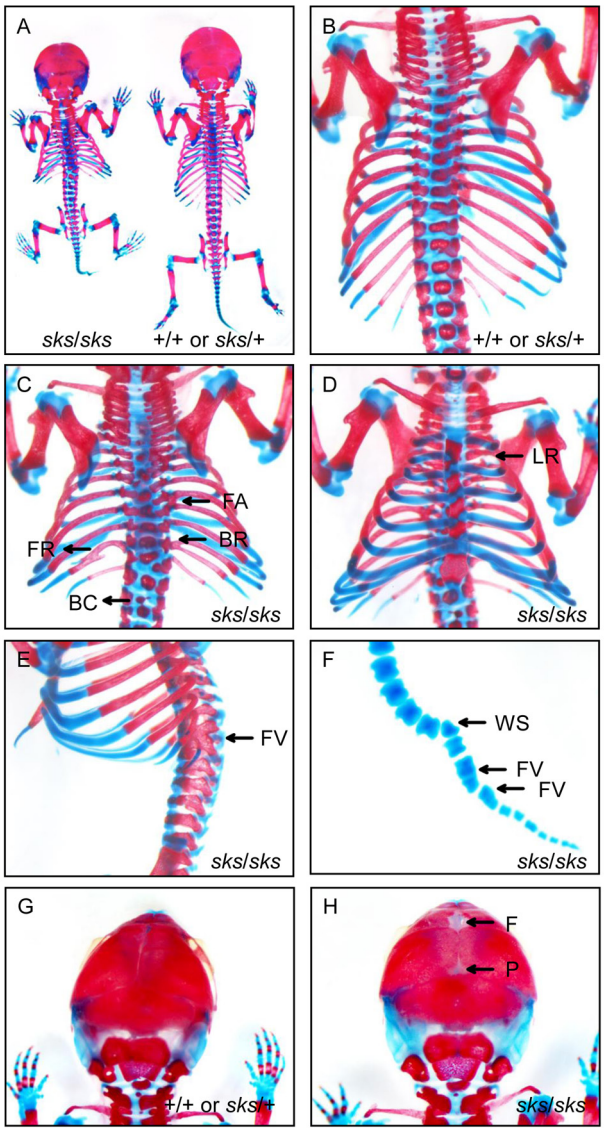

Fig. 3. Skeletal defects of *sks* mutant mice at the neonatal stage. (A) Whole skeleton, (B, C, D, E) thoracic region, (F) coccygeal region, and (G, H) dorsal skull bones of alizarin red– and alcian blue–stained skeletal preparations of 1-day-old newborn mutant (*sks*/*sks*) and normal (*sks*/+ or +/+) mice. Skeletal malformations are indicated as FR, fused rib; FA, fused arch; BR, branched rib; BC, bipartite centra; LR, loss of rib; WS, wedge-shaped pieces of bone; and FV, fused vertebrate. Note the smaller size of the (F) frontal and (P) parietal bones.

Developmental defects of the axial skeleton in sks/sks embryos

To determine when and how skeletal abnormality of *sks*/*sks* mice appears during embryonic development, we examined hematoxylin and eosin (H&E)-stained histological sections of embryos taken at embryonic day E11.5 and E12.5 and alcian blue-stained whole embryos at E14.5. As shown in Fig. 4B, normal somite formation was observed in the E11.5 *sks*/*sks* embryos with no apparent morphological difference compared with the *sks*/+ or +/+ embryos. This suggests normal formation and segmentation of the sclerotome, which gives rise to the axial skeleton. However, at E12.5, vertebral malformations showing disorganized vertebrae appeared on the prospective cervical and thoracic regions of the *sks*/*sks* embryos (Fig. 4C and E). As a result, a bent neural tube was observed in *sks*/*sks* embryos, while that of *sks*/+ or +/+ embryos was straight (Fig. 4D and F). At E14.5, fusions and/or bifurcations of the axial skeletal elements and irregular intervertebral spaces were observed in the thoracic vertebrae and ribs of the *sks*/*sks* embryos (Fig. 4G and H). Since cartilaginous vertebrae and rib primor-

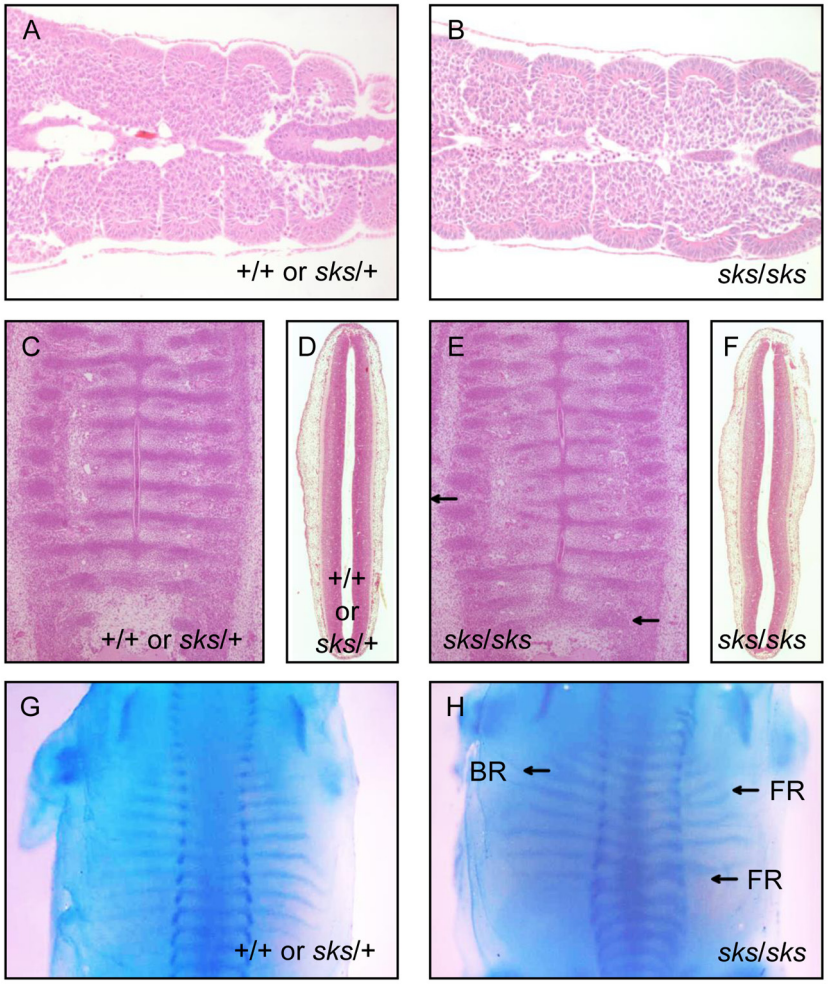

Fig. 4. Multiple skeletal defects of *sks* mutant mice at embryonic stages. (A, B) Dorsal sections of tail of the embryos at E11.5. (C, E) Dorsal sections of prospective cervical and thoracic regions of embryos at E12.5. (D, F) Dorsal sections of the neural tube of embryos at E12.5. (G, H) Alcian blue–stained skeletal preparations of mutant and normal mice at embryonic stage E14.5. Skeletal malformations are indicated as FR, fused rib, and BR, branched rib. Vertebral malformations are indicated by arrows.

dia had formed but ossification had not initiated at E12.5, the defects of the axial skeleton observed in the *sks*/*sks* mice may have been caused by malformation of the cartilaginous vertebrae and ribs at an early developmental stage after somite formation and segmentation.

Lethality of sks/sks mice

Out of 251 mice obtained from mating between *sks*/+ males and females of the *sks* strain, 27 *sks/sks* mice were still alive at the weaning (P20) (Table 1). This was significantly lower than expected based on Mendelian segregation ($P<0.005$). Furthermore, the sex ratio of *sks*/*sks* mice also deviated from expectation ($P<0.05$) at P20 (Table 1). These findings indicate that more than 50% of *sks*/*sks* mice, and females in particular, died before weaning. Therefore, we collected embryos from mating between *sks*/+ mice at different embryonic stages and determined the genotype. As shown in Table 1, the proportion of *sks*/*sks* embryos was lower than the expected ratio of 1:3 at E10.5, 12.5, 14.5, and 16.5, but the difference was not statistically significant. Since no apparent deaths during lactation were observed, these findings suggest that a considerable number of *sks*/*sks* mice died just after and/or before birth. The cause of neonatal and/or prenatal death in *sks*/*sks* mice is unclear, but severe skeletal aberrations, particularly of the thoracic region,

Table 1. Frequency of genotypes obtained from intercrossing sks heterozygous mice

	Number of litters	Average of litter size	SEM	Genotype	
				sks/*sks*	*sks*/+, +/+
P20	56	4.48	0.21	27* (20:7**)	224 (111:113)
E16.5	4	5.75	0.63	5 (4:1)	18 (12:6)
E14.5	4	7.50	0.63	6 (3:3)	24 (11:13)
E12.5	4	6.75	1.12	3 (1:2)	24 (12:12)
E10.5	2	10.0	0.00	4 (2:2)	16 (7:9)

*Significantly difference from the expected ratio (χ^2=27.17, P<0.005). The ratio of males to females is shown in parentheses. ** Significantly difference from the expected sex ratio (χ^2=6.26, P<0.05).

could be a possible cause, since defects of the respiratory system are a common cause of neonatal death in mice.

Linkage mapping of the sks locus

We used linkage analysis to determine the precise chromosomal location of the *sks* locus. A total of 532 F_2 progeny, including 63 *sks*/*sks* and 469 *sks*/+ or +/+ mice, were obtained from intercrossing *sks*/+ F_1 mice from a cross between *sks* and JF1/Ms mice. The *sks* locus has been roughly mapped to chromosome 4, distal to the *Tyrp1* gene. Therefore, we genotyped the 63 *sks*/*sks* mice for 7 microsatellite makers located in that region of chromosome 4. As shown in Fig. 5A, we observed 3 and 1 recombination events between the *sks* locus and *D4Mit331* and *D4Mit199*, respectively. No recombination was observed between *sks* and *D4Mit31* or *D4Mit1146*. These segregation data indicated that the *sks* locus is located within an approximately 8-Mb interval between *D4Mit331* and *D4Mit199* on mouse chromosome 4 (Fig. 5B).

Discussion

Handel *et al.* [13] reported that adult *sks*/*sks* mice show skeletal fusions of the cervical, thoracic, lumbar, and caudal vertebrae and bilateral or unilateral fusions of the ribs. Our findings regarding the axial skeleton are essentially in concordant with these previously reported skeletal abnormalities, but we also found polydactyly and delayed skull ossification in the *sks*/*sks* mice in the present study. We also found that the abnormalities of the axial skeleton in the adult mice were already apparent in the neonates. In particular, we found irregular formation of cartilaginous caudal vertebrae and disorganized ossification of vertebrae in the neonatal *sks*/*sks* mice. These findings suggest that morphological abnormalities observed in *sks*/*sks* mice are caused by defects in the formation of cartilaginous vertebrae. We, therefore, investigated axial skeleton formation during embryonic development and found that the skeletal defects, including fusions and/or bifurcations of the axial skeletal elements and irregular intervertebral spaces, were observed in E12.5 and E14.5 embryos but not in E11.5 embryos. This indicates that malformation of the axial skeleton appears prior to the initiation of vertebral and rib ossification but after segmentation of the somites.

Many mutant mice having a kinky tail have been reported. However, the phenotypes of these mutant mice differ from that of *sks* mice. For example, Kusumi *et al.* [18], Dunwoodie *et al.* [6], and Shinkai *et al.* [23] reported a short trunk and short, kinky tail in mice with a mutation of the delta-like 3 (Drosophila) (*Dll3*) gene. Neonatal *Dll3*$^{-/-}$ mice have a highly disorganized axial skeleton with numerous vertebral and rib fusions, and the underlying phenotype is suggested to be a defectively formed and segmented sclerotome caused by patterning defects of somitogenesis. *Dll3* is one of the ligands for Notch [5]. In mammals, somite segmentation is the initial step of axial skeleton formation and relies on boundary formation in the presomitic mesoderm, which is controlled by the Notch signaling pathway [1, 8]. Therefore, loss of *Dll3* gene function causes vertebral defects due to defective formation of the morphological borders between somites by E9.5 during embryogenesis [6, 18]. On the other hand, the mutant mouse possessing the insertional mutation of the *Skt* gene shows compression of the tail bud intervertebral discs (IVDs) at E17.5, resulting in a kinky-tail phenotype [22]. The *Skt* mouse shows no abnormality in the vertebral region up to E16.5, and IVD compression first appears at E17.5. In the adult mouse, shortened and curved caudal vertebrae are re-

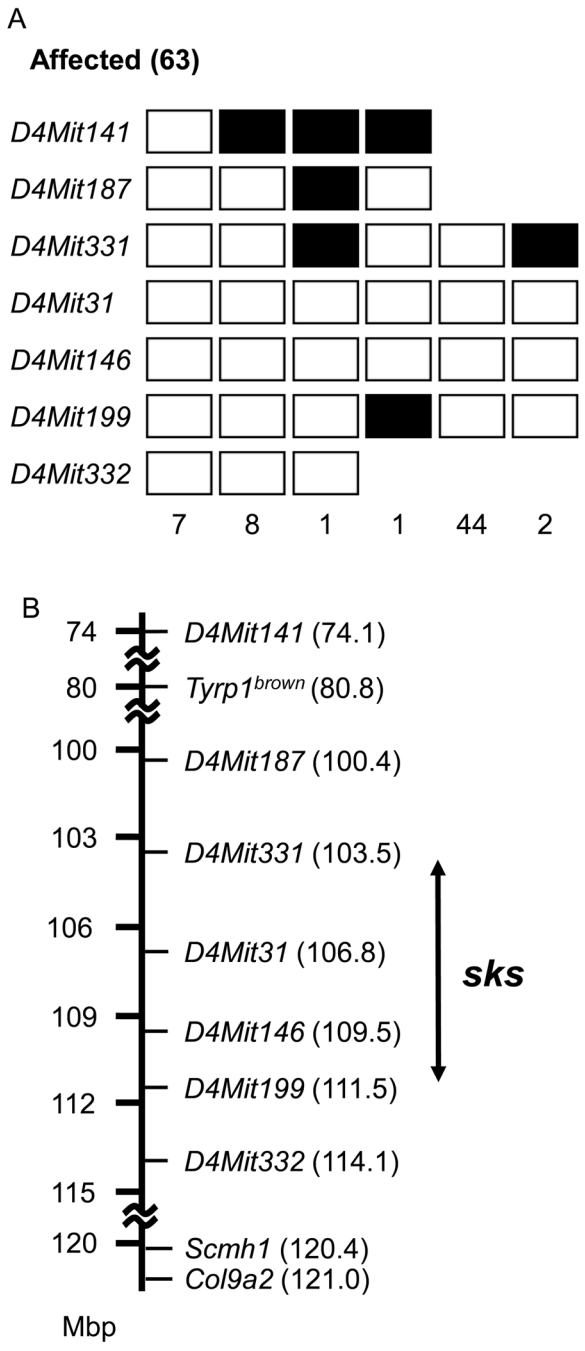

Fig. 5. Localization of the *sks* locus on mouse chromosome 4. (A) Segregation of haplotypes in 63 F_2 affected mice obtained from crosses between *sks* and JF1/ms mice. Open boxes represent the *sks* alleles. Filled boxes represent the presence of JF1/MS type alleles. The number of F_2 mice carrying each haplotype is indicated at the bottom of the columns. (B) A map of mouse chromosome 4 showing the location of the *sks* locus. The positions of microsatellite markers in the critical region are indicated in Mb according to the mouse genome sequence (Annotation Release 103, GRCm38.p1, accession GCF 000001635.21), and the *sks* locus is indicated by an arrow.

stricted to the 20th–25th caudal vertebrae, and no other skeletal abnormality is observed. These examples illustrate the relationship between the developmental stage at which defects first appear and the types and severity of skeletal abnormalities. *Dll3*$^{-/-}$ mice shows vertebral and rib fusion across the entire axial skeleton, and the defect appears at E9.5; the *Skt* mouse shows shortened and curved vertebrae restricted to the posterior caudal vertebrae, and the defect appears at E17.5. In contrast, the *sks* mouse shows fusion of vertebrae and ribs across the entire axial skeleton, which is apparently milder than that of *Dll3*$^{-/-}$ mice, and the defect appears at E12.5. Since the skeletal phenotype of *sks* is unique compared with those of other mutant mice with defective axial skeletons, *sks* mice may prove to be a good model for investigating the developmental mechanisms associated with the axial skeletal formation of mammals.

One obvious difference of the *sks* mouse from other mutant mice with skeletal defects is the sterility due to defective gametogenesis. The *sks*/*sks* mouse is subject to defective pairing of homologous chromosomes and formation of the synaptonemal complex during the prophase I of meiosis in spermatogenesis [13]. Therefore, the gene for the *sks* mutation has been predicted to play an essential role in meiosis. Although mice with a mutation for LFNG O-fucosylpeptide 3-beta-N-acetylglucosaminyltransferase (*Lfng*), which functions in the development of the axial skeleton, including somite formation [7, 30], also show sterility caused by defective folliculogenesis in females [12], no mutant mice other than *sks* mcie have been reported to show defects in both axial skeletal formation and gametogenesis. However, there is a possibility that two closely localized genes associated with skeletal development and/or gametogenesis are simultaneously disrupted by a large deletion, *sks* mice will be a useful model for investigating processes common to both axial skeleton development and meiosis during gametogenesis. Spondylocostal dysostosis is a human inherited disorder characterized by short trunk, mild scoliosis, defects in vertebral segmentation, and fusions and deletions of ribs [29]. The cause in some of the patients with this disorder has been reported to be mutations in genes involved in the Notch signaling pathway including DLL3 and LFNG [29], but the causes in the remaining patients with this disorder remain unknown. Since the skeletal abnormalities of *sks* mice resemble to those of spondylocostal dysostosis, the gene responsible for the *sks* mutation might also be involved

in this human disorder, and *sks* mice can be good animal model for this human disorder.

We mapped the *sks* locus to an 8-Mb region of mouse chromosome 4 by linkage analysis. At least 95 genes are located within this interval, including 71 genes with known function, 11 predicted genes with unknown function, and 14 pseudogenes. None of the genes reported for this region are known to be involved in skeletal formation and gametogenesis, but the expression patterns of these 71 positional candidate genes obtained from the NCBI UniGene database indicate expression of 20 out of the 71 genes in the testis, ovary, and developing embryo. Therefore, these 20 genes including basic transcription factor 3-like 4 (*Btf3l4*) and epidermal growth factor receptor pathway substrate 15 (*Eps15*) are potential candidate genes. Furthermore, the mapping results exclude 2 strong candidate genes, collagen, type IX, alpha 2 (*Col9A2*) and sex comb on midleg homolog 1 (*Scmh1*), both located on chromosome 4, distal to the *b* gene [9, 26]. A mutation in the human homolog of the *Col9A2* gene causes multiple epiphyseal dysplasia type 2 [20] resulting in hypoplasia of anterior vertebral elements [2]. The *Scmh1* gene encodes a constituent of Polycomb repressive complex 1; the SCMH1 null mutant exhibits skeletal abnormality of the axis and male sterility due to defects of chromatin modification [25]. However, both *Col9a2* and *Scmh1* are outside of the 8-Mb region defined by these linkage analyses and can be excluded from the candidate genes (Fig. 5B). Fine mapping and positional cloning of the *sks* locus will be necessary to identify the novel gene (s) essential for axial skeletal formation and/or gametogenesis.

Acknowledgments

This work was supported by grants from the Japan Society for the Promotion of Science and the Sasakawa Science Research Grant from the Japan Science Society (18-130).

References

1. Barrantes, I.B., Elia, A.J., Wünsch, K., Hrabe de Angelis, M.H., Mak, T.W., Rossant, J., Conlon, R.A., Gossler, A., and de la Pompa, J.L. 1999. Interaction between Notch signalling and Lunatic fringe during somite boundary formation in the mouse. *Curr. Biol*. 9: 470–480. [Medline] [CrossRef]
2. Briggs, M.D., Choi, H., Warman, M.L., Loughlin, J.A., Wordsworth, P., Sykes, B.C., Irven, C.M., Smith, M., Wynne-Davies, R., Lipson, M.H., Biesecker, L.G., Garber, A.P., Lachman, R., Olsen, B.R., Rimoin, D.L., and Cohn, D.H. 1994. Genetic mapping of a locus for multiple epiphyseal dysplasia (EDM2) to a region of chromosome 1 containing a type IX collagen gene. *Am. J. Hum. Genet*. 55: 678–684. [Medline]
3. Chuma, S. and Natatsuji, N. 2001. Autonomous transition into meiosis of mouse fetal germ cells *in vitro* and its inhibition by gp130-mediated signaling. *Dev. Biol*. 229: 468–479. [Medline] [CrossRef]
4. Dobrovolskaïa-Zavadskaïa, N. 1927. Sur la mortification spontnée de la queue chez la souris nouveau-née et sur l'existence d'un caractere (facteur) héréditaire "non-viable". *Crit. Rev. Seance Soc. Biol*. 97: 114–116.
5. Dunwoodie, S.L., Henrique, D., Harrison, S.M., and Beddington, R.S. 1997. Mouse *Dll3*: a novel divergent Delta gene which may complement the function of other Delta homologues during early pattern formation in the mouse embryo. *Development* 124: 3065–3076. [Medline]
6. Dunwoodie, S.L., Clements, M., Sparrow, D.B., Sa, X., Conlon, R.A., and Beddington, R.S. 2002. Axial skeletal defects caused by mutation in the spondylocostal dysplasia/pudgy gene *Dll3* are associated with disruption of the segmentation clock within the presomitic mesoderm. *Development* 129: 1795–1806. [Medline]
7. Evrard, Y.A., Lun, Y., Aulehla, A., Gan, L., and Johnson, R.L. 1998. *lunatic fringe* is an essential mediator of somite segmentation and patterning. *Nature* 394: 377–381. [Medline]
8. Forsberg, H., Crozet, F., and Brown, N.A. 1998. Waves of mouse *Lunatic fringe* expression, four-hour cycles at two-hour intervals, precede somite boundary formation. *Curr. Biol*. 8: 1027–1030. [Medline] [CrossRef]
9. Giampietro, P.F., Raggio, C.L., and Blank, R.D. 1999. Synteny-defined candidate genes for congenital and idiopathic scoliosis. *Am. J. Med. Genet*. 83: 164–177. [Medline] [CrossRef]
10. Grüneberg, H. 1954. Genetical studies on the skeleton of mouse. XIII. Curly-tail. *J. Genet*. 52: 52–67. [CrossRef]
11. Grüneberg, H. 1961. Genetical studies on the skeleton of mouse. XXIX. Pudgy. *Genet. Res*. 2: 384–393. [CrossRef]
12. Hahn, K.L., Johnson, J., Beres, B.J., Howard, S., and Wilson-Rawls, J. 2005. Lunatic fringe null female mice are infertile due to defects in meiotic maturation. *Development* 132: 817–828. [Medline] [CrossRef]
13. Handel, M.A., Lane, P.W., Schroedar, A.C., and Davisson, M.T. 1988. New mutation causing sterility in the mouse. *Gamete. Res*. 21: 409–423. [Medline] [CrossRef]
14. Herrmann, B.G., Labeit, S., Poustka, A., King, T.R., and Lehrach, H. 1990. Cloning of the *T* gene required in mesoderm formation in the mouse. *Nature* 343: 617–622. [Medline] [CrossRef]
15. Johnson, D.R. and Wallace, M.E. 1979. Crinkly-tail, a mild skeletal mutat in the mouse. *J. Embryol. Exp. Morphol*. 53: 327–333. [Medline]
16. Johnson, J., Rhee, J., Parsons, S.M., Brown, D., Olson, E.N., and Rawls, A. 2001. The anterior/posterior polarity of somites is disrupted in paraxis-defcient mice. *Dev. Biol*. 229:

176–187. [Medline] [CrossRef]
17. Koizumi, K., Nakajima, M., Yuasa, S., Saga, Y., Sakai, T., Kuriyama, T., Shirasawa, T., and Koseki, H. 2001. The role of presenilin 1 during somite segmentation. *Development* 128: 1391–1402. [Medline]
18. Kusumi, K., Sun, E.S., Kerrebrock, A.W., Bronson, R.T., Chi, D.C., Bulotsky, M.S., Spencer, J.B., Birren, B.W., Frankel, W.N., and Lander, E.S. 1998. The mouse pudgy mutation disrupts *Delta* homologue *Dll3* and initiation of early somite boundaries. *Nat. Genet*. 19: 274–278. [Medline] [CrossRef]
19. Morgan, W.C. 1950. A new tail-short mutation in the mouse whose lethal effects are conditioned by the residual genotypes. *J. Hered*. 41: 208–215. [Medline]
20. Muragaki, Y., Mariman, E.C., van Beersum, S.E., Perala, M., van Mourik, J.B., Warman, M.L., Olsen, B.R., and Hamel, B.C. 1996. A mutation in the gene encoding the alpha 2 chain of the fibril-associated collagen IX, COL9A2, causes multiple epiphyseal dysplasia (EDM2). *Nat. Genet*. 12: 103–105. [Medline] [CrossRef]
21. Pourquie, O. 2000. Segmentation of the paraxial mesoderm and vertebrate somitogenesis. *Curr. Top Dev. Biol*. 47: 81–105. [Medline] [CrossRef]
22. Semba, K., Araki, K., Li, Z., Matsumoto, K., Suzuki, M., Nakagata, N., Takagi, K., Takeya, M., Yoshinobu, K., Araki, M., Imai, K., Abe, K., and Yamamura, K. 2006. A novel murine gene, Sickle tail, linked to the Danforth's short tail locus, is required for normal development of the intervertebral disc. *Genetics* 172: 445–456. [Medline] [CrossRef]
23. Shinkai, Y., Tsuji, T., Kawamoto, Y., and Kunieda, T. 2004. New mutant mouse with skeletal deformities caused by mutation in delta like 3 (*Dll3*) gene. *Exp. Anim*. 53: 129–136. [Medline] [CrossRef]
24. Silver, L.M. 1985. Mouse t haplotype. *Annu. Rev. Genet*. 19: 179–208. [Medline] [CrossRef]
25. Takada, Y., Isono, K., Shinga, J., Turner, J.M., Kitamura, H., Ohara, O., Watanabe, G., Singh, P.B., Kamijo, T., Jenuwein, T., Burgoyne, P.S., and Koseki, H. 2007. Mammalian Polycomb Scmh1 mediates exclusion of Polycomb complexes from the XY body in the pachytene spermatocytes. *Development* 134: 579–590. [Medline] [CrossRef]
26. Tomotsune, D., Takihara, Y., Berger, J., Duhl, D., Joo, S., Kyba, M., Shirai, M., Ohta, H., Matsuda, Y., Honda, B.M., Simon, J., Shimada, K., Brock, H.W., and Randazzo, F. 1999. A novel member of murine Polycomb-group proteins, Sex comb on midleg homolog protein, is highly conserved, and interacts with RAE28/mph1 in vitro. *Differentiation* 65: 229–239. [Medline] [CrossRef]
27. Wright, M.E. 1947. Undulated: a new genetic factor in Mus musculus affecting the spine and tail. *Heredity* 1: 137–141. [CrossRef]
28. Yoon, J.K. and Wold, B. 2000. The bHLH regulator pMesogenin1 is required for maturation and segmentation of paraxial mesoderm. *Genes Dev*. 14: 3204–3214. [Medline] [CrossRef]
29. Zanotti, S. and Canalis, E. 2013. Mechanisms in Endocrinology: Notch signaling in skeletal health and disease. *Eur. J. Endocrinol*. 168: R95–R103. [Medline] [CrossRef]
30. Zhang, N. and Gridley, T. 1998. Defects in somite formation in *lunatic fringe*-deficient mice. *Nature* 394: 374–377. [Medline]